Carbohydrate Polymers 86 (2011) 192–201

Contents lists available at ScienceDirect

Carbohydrate Polymers

journal homepage: www.elsevier.com/locate/carbpol

Nanoreinforced biocompatible hydrogels from wood hemicelluloses and cellulose whiskers

Muzaffer Ahmet Karaaslan[a], Mandla A. Tshabalala[b], Daniel J. Yelle[b], Gisela Buschle-Diller[a,*]

[a] Department of Polymer and Fiber Engineering, Auburn University, Auburn, AL 36849-5327, United States
[b] USDA Forest Products Laboratory, One Gifford Pinchot Drive, Madison, WI 53726, United States

ARTICLE INFO

Article history:
Received 2 February 2011
Received in revised form 13 April 2011
Accepted 14 April 2011
Available online 21 April 2011

Keywords:
Hemicellulose
Cellulose whiskers
PHEMA
Hydrogel
Articular cartilage

ABSTRACT

Nanoreinforced hydrogels with a unique network structure were prepared from wood cellulose whiskers coated with chemically modified wood hemicelluloses. The hemicelluloses were modified with 2-hydroxyethylmethacrylate prior to adsorption onto the cellulose whiskers in aqueous medium. Synthesis of the hydrogels was accomplished by *in situ* radical polymerization of the methacrylic groups of the adsorbed coating to form a network of poly(2-hydroxyethylmethacrylate) (PHEMA) matrix reinforced with cellulose whiskers. The mechanical, swelling and viscoelastic properties, of water-swollen hydrogels were investigated. Results indicated that the number of effective crosslinks between polymer chains and the average chain length between crosslinking points was significantly different from PHEMA hydrogels that had been crosslinked by a conventional chemical method, using a cross-linking agent. The resulting hydrogels had enhanced toughness, increased viscoelasticity, and improved recovery behavior. With respect to the mechanical and swelling properties, it can be hypothesized that these nanoreinforced PHEMA hydrogels have potential for use in load-bearing biomedical applications such as articular cartilage replacement.

Published by Elsevier Ltd.

1. Introduction

Polymers from renewable resources are receiving increased attention in the scientific community because of projected shortage of petroleum-based raw materials in the near future. Tremendous effort is focused on the development of new materials and processes that could replace synthetic polymers by bio-based polymers as viable alternatives.

Polysaccharides have been used in a wide range of applications such as food, packaging, agricultural chemicals, and biomedical devices where non-toxicity, biocompatibility and biofunctionality are required. Cellulose and its derivatives have been utilized extensively as textile fibers, chemical precursors and for paper making and food additives. Cellulose whiskers (nanocrystals), obtained by acid hydrolysis of cellulose, are a more recent area of application for nanocomposites (Habibi, Lucia, & Rojas, 2010). In the acid hydrolysis process, the amorphous regions of cellulose are dissolved, yielding crystalline rod or whisker shape nanoparticles with diameters that range from 8 to 20 nm and lengths of 100 nm to few micrometers, depending on the source of the cellulose (Lima & Borsali, 2004). These whiskers have a high modulus, high aspect ratio, and their surface chemistry can be modified to broaden their use in high-value applications (Samir, Alloin, & Dufresne, 2005).

Hemicelluloses are hetero-polysaccharides, representing about 20–35% of lignocellulosic biomass, and are present in the cell wall of wood and annual plants together with cellulose and lignin (Gatenholm & Tenkanen, 2004). Despite their abundance in nature, they have been under-utilized commercially. Recent research efforts are focused on their application in hydrogels for biomedical applications because of their biodegradability and hydrophilicity (Ebringerova, 2006). Utilizing the strong natural hemicellulose–cellulose interaction, novel functionalities have been introduced on cellulose surfaces without degrading its morphology and native structure (Zhou, Rutland, Teeri, & Brumer, 2007). Xylan is one of the most common hemicelluloses and its barrier properties for food packaging applications have been studied extensively. Recent studies have shown that, when reinforced with cellulose nanowhiskers, xylan composite films could have significantly improved water barrier properties, tensile strength, and tensile energy absorption (Saxena, Elder, Pan, & Ragauskas, 2009; Saxena, Elder, & Ragauskas, 2011). These improvements were attributed to a rigid hydrogen-bonded network of nanowhiskers in the xylan matrix and strong cellulose/xylan interactions.

Hydrogels are crosslinked networks of hydrophilic polymers that are capable of retaining considerable amounts of water without disintegration. In addition to their high water up-take, stimuli-responsive swelling capabilities and biocompatibility are

* Corresponding author. Tel.: +1 3348445468; fax: +1 3348444068.
E-mail address: buschgi@auburn.edu (G. Buschle-Diller).

0144-8617/$ – see front matter. Published by Elsevier Ltd.
doi:10.1016/j.carbpol.2011.04.030

some of the features that render them suitable for biological and biomedical applications (Peppas, Hilt, Khademhosseini, & Langer, 2006; Slaughter, Khurshid, Fisher, Khademhosseini, & Peppas, 2009). However, it has been a challenge to fabricate mechanically strong hydrogels by conventional chemical crosslinking pathways without compromising their other properties such as water uptake and stimuli responsiveness (Haraguchi, Takehisa, & Fan, 2002). Recently, nanocomposite hydrogels (NC gels) were developed with unique organic–inorganic network structures that exhibit excellent mechanical performance as well as optical and swelling/deswelling properties (Haraguchi & Takehisa, 2002). In their study, water-swellable clay nanosheets were used as highly multifunctional crosslinking sites. By performing *in situ* polymerization of specific monomers, initiators attached to nanoclay surfaces were used as grafting sites for growing polymer chains. As a consequence, long and extensible polymer chains formed, connecting the uniformly distributed nanoclay particles to each other. NC gels were described as strong, tough, highly extensible, optically transparent and capable of absorbing higher amounts of water compared to conventional hydrogels. In another study, Huang et al. (2007) synthesized novel high strength hydrogels (MMC gels) using a similar approach to NC gels. A suspension of macromolecular microspheres carrying peroxide groups were irradiated to initiate polymerization of monomers and to synthesize hydrogels. The network structure of these hydrogels showed similarities to NC gels. One common potential use for such hydrogels with high mechanical performance is as synthetic substitutes for damaged articular cartilage which is a load-bearing natural tissue within joints in the human body. Articular cartilage is a viscoelastic material showing non-linear strain response and is considered a natural hydrogel consisting of 65–85% water in its structure (Boschetti, Pennati, Gervaso, Peretti, & Dubini, 2004). Elastic modulus and fracture stress of human cartilage depend on its location in the body. It has been reported that elastic modulus of cartilage is in the range of 0.4–10 MPa and fracture stress is 78.6 MPa at 99.3% compressive strain (Huang et al., 2007; Millon, Oates, & Wan, 2009).

The objective of this study was to design novel hydrogels with improved mechanical properties by utilizing hemicellulose and cellulose whiskers derived from wood. Hemicellulose, isolated from aspen wood, was chemically modified with 2-hydroxyethylmethacrylate (HEMA) prior to adsorption onto cellulose whiskers. The surface modified cellulose whiskers were used to prepare nanocomposite hydrogels using free radical polymerization of HEMA, a common biocompatible monomer. The effect of morphology and concentration of the incorporated nanocrystals on the mechanical, viscoelastic, and swelling properties of the resulting hydrogels was investigated. An attempt was made to achieve mechanical and viscoelastic properties of the resulting hydrogels that would make them a potential replacement material for articular cartilage.

2. Experimental

2.1. Materials

96% pure 2-hydroxyethyl methacrylate (HEMA) monomer was purchased from Acros Chemicals. To remove impurities such as ethylene glycol dimethacrylate, further purification was performed as described elsewhere (Bryant, Janet, Hauch, & Ratner, 2007). Dimethyl sulfoxide (DMSO), chloroform, acetone, sulfuric acid, ethyl acetate, ammonium persulfate, sodium pyrosulfite, ethylene glycol dimethacrylate (EGDMA), N,N′-carbonyldiimidazole (CDI) and triethylamine were obtained from Sigma–Aldrich and used as received. Whatman filter paper #1 (Fisher Chemicals) served as the source for cellulose nanowhiskers (CNW) control samples.

2.2. Hemicellulose extraction from aspen

Hemicellulose was provided by USDA Forest Products Laboratory, Madison, WI. Hemicellulose was isolated from fresh milled aspen chips by extraction under mild alkaline conditions. The detailed procedure has been described in Karaaslan, Tshabalala, & Buschle-Diller (2010).

2.3. Preparation of cellulose nanowhiskers

CNW were prepared by acid hydrolysis of cellulose from two different sources; aspen wood cellulose and cotton cellulose (filter paper #1). After grinding in a Wiley mill, cellulose powder was hydrolysed under constant stirring at 45 °C for 45 min using sulfuric acid (64 wt%) at 17.5 mL/g acid-to-pulp ratio according to the procedure described elsewhere (Beck-Candanedo, Roman, & Gray, 2005; Dong, Revol, & Gray, 1998). To stop the hydrolysis reaction, 10-fold excess of deionized (DI) water was added. The suspensions were centrifuged and the acid residue was decanted. After washing the precipitate and redispersing in DI water, the CNW suspension was dialysed against DI water using a dialysis membrane with 13,000 molecular weight cut-off. The dialysis was continued for 3–5 days, until the pH of the solution remained constant at pH $\geq$5.0. Finally, aqueous CNW suspensions were sonicated for 10 min at 30% output control in an ice-cold water bath. A drop of chloroform was added to prevent bacterial growth and the suspension was stored in a refrigerator. The concentrations of CNW suspensions were determined gravimetrically. The concentration of sulfate groups for the starting CNWs isolated from aspen wood was determined by conductometric titration according to the method developed by Araki, Wada, Kuga, & Okano (1998) and was found to be 65 mmol/kg.

2.4. Preparation of CNW coated with HEMA-modified hemicellulose and hydrogel formation by polymerization of HEMA

Hemicellulose was first modified with HEMA monomer, adsorbed onto CNW and HEMA polymerized to form a hydrogel, as described in the following sections.

2.4.1. Chemical modification of hemicellulose

Hemicellulose with methacrylic functionality was synthesized according to Lindblad, Ranucci, & Albertsson (2001) with slight modifications. Briefly, 286 mg aspen hemicellulose and 456 mg 2-[(1-imidazolyl)formyloxy]ethyl methacrylate (HEMA-Im) were mixed in DMSO and triethylamine (40.5 mg) was added as the catalyst. Two different batches were prepared in which the reaction was kept at 45 °C under stirring for 10 and 25 h, respectively. 10 h and 25 h batches are hereafter referred to as MH-10 and MH-25. The product was precipitated twice in ethyl acetate, centrifuged, the solvent was decanted and the final precipitate freeze-dried overnight.

2.4.2. Adsorption of modified hemicellulose to CNW

Adsorption experiments were performed according to a modified method described for the adsorption of cationized glucoronoxylans on softwood cellulose fibers (Köhnke, Brelid, & Westman, 2009). Aqueous MH-10 solution (0.4 mL; 1%) was mixed with 2 mL of a CNW aqueous suspension (1%, w/v) and 0.05 mL 0.5 M NaCl in a vial resulting in a final concentration of 10 mM NaCl and 200 mg/g MH:CNW ratio. In the case of MH-25, 0.8 mL of a 0.5% aqueous solution of MH-25 was used with the concentration of the other components remaining the same. The vials were sealed with parafilm and incubated in an oven at 45 °C for 24 h. Non-adsorbed MH was separated from the MH-coated CNW suspensions by solvent exchange with acetone according to the procedure described elsewhere (Capadona et al., 2007). After a mechanically coherent

CNW organogel layer had formed, the acetone/water mixture at the top of CNW layer was collected and stored in a beaker. Finally, the separated mixture was flushed with nitrogen to remove acetone. The remaining aqueous solution was used to determine the non-adsorbed to adsorbed amount of MH.

2.4.3. Hydrogel synthesis by polymerization of HEMA

Free radical polymerization of HEMA in water via redox initiators was performed to synthesize nanoreinforced PHEMA hydrogels (NR-PHEMA) using the monomer/water/initiator ratios reported in a recent study (Lindblad, Albertsson, Ranucci, Laus, & Giani, 2005). MH-coated CNW, in the form of organogels (acetone gels), were redispersed in DI water and flushed with nitrogen to remove acetone. 500 mg of HEMA monomer was added to 250 μL of the MH-coated CNW suspension at different compositions (0.2%, 1% and 2%, w/v) and vortexed. After adding the initiator (12.5 μL each of 4% (w/v) ammonium persulfate and sodium pyrosulfite aqueous solutions, respectively), the polymerizing solution was vortexed and immediately poured into a glass vial, flushed with nitrogen and sealed with parafilm. *In situ* polymerization was maintained for 3 h in an oven at 40 °C. To remove unreacted monomers and initiators and allow hydrogels to reach their equilibrium swelling, the synthesized hydrogels were immersed in excess DI water for 5 days by exchanging with fresh water 1–2 times daily. Final CNW weight fraction (w/w, %) in hydrogels was calculated by the ratio of CNW to initial monomer.

Control samples, normal structure hydrogels (NS-PHEMA gels), which were crosslinked by a conventional chemical crosslinking agent using EGDMA, were also prepared. The weight fraction of the cross linker was 1% with respect to the amount of HEMA.

2.5. Characterization

2.5.1. Morphology of cellulose whiskers

The morphology of CNW was evaluated by Transmission Electron Microscopy (TEM). 20 μL of CNW dispersion (0.01%, w/v) was placed on a 300 mesh carbon film coated copper grid and air dried. Enhanced image contrast was obtained by negative staining with uranyl acetate. The aspect ratio (L/d) of CNW was determined by using Adobe Photoshop 7.0. Average values of length and width of at least 15 individual whiskers were reported.

2.5.2. Structure of hemicellulose isolate

Two-dimensional (2-D) ^{1}H ^{13}C NMR spectra of the hemicellulose isolate were acquired on a Bruker–Biospin (Rheinstetten, Germany) AVANCE 500 MHz spectrometer fitted with a cryogenically cooled 5-mm Bruker TCI gradient probe with inverse geometry. Heteronuclear Single Quantum Coherence (HSQC) and Heteronuclear Multiple Bond Correlation (HMBC) spectra, for one-bond ^{13}C–^{1}H correlations and long-range ^{13}C–^{1}H correlation, respectively, were acquired. Prior to Fourier transformation, the data matrices were zero-filled to 1024 points in the ^{13}C dimension. To determine connectivity of the xylan structure, Nuclear Overhauser Effect Spectroscopy (NOESY) experiments were performed, which were used to characterize the glucuronoxylan structure through space. NOESY enables ^{1}H nuclei that are near each other in space to be detected; cross-peaks occur between atoms that are near to each other, whether they are coupled or not.

2.5.3. Degree of modification of hemicellulose

Analysis of modified hemicellulose was performed by FT-IR and ^{1}H NMR spectroscopy. The degree of modification (D_m) was determined by using specific chemical shifts of the ^{1}H NMR spectrum (Fig. 3a). D_m, the relative ratio of the vinyl C–H peaks (δ = 5.7 and 6.07 ppm) on methacrylated hydroxyl groups to the broad peaks (δ = 3.2–5.5 ppm) from the hemicellulose backbone, was estimated by using Eq. (1) in accordance with the method used for acetylated hemicelluloses (Gröndahl, Teleman, & Gatenholm, 2003);

$$D_m = \frac{\text{Sum of integrals of methacrylated hydroxyl groups } (\delta = 5.7 \text{ ppm and } 6.07 \text{ ppm})/2}{\text{Sum of integrals of all carbohydrate signals } (\delta = 3.2 - 5.5 \text{ ppm})/6} \quad (1)$$

2.5.4. Degree of adsorption of methacrylated hemicellulose on CNW

Iodine complexation (Köhnke et al., 2009; Gaillard & Thompson, 1971) was used to estimate the amount of MH adsorbed to CNW. 0.1 mL of MH solution was mixed with 0.4 mL of DI water, 4 mL of 4.62 M $CaCl_2$ and 0.5 mL of triiodine stock solution (0.5% I_2 + 2.1% KI). Absorbance at 610 nm was recorded with an UV–Vis spectrophotometer. The amount of adsorbed MH was calculated using a standard curve of known concentrations of MH aqueous solutions. To evaluate the contribution of CNW to the absorbance at 610 nm of MH solutions, control samples of CNW suspensions with and without MH were also analysed. Non-MH-coated CNW suspensions did not form colored iodine complexes and their contribution at 610 nm was negligible.

2.5.5. Hydrogel characterization

The equilibrium swelling ratio (S) was calculated by the following equation (Eq. (2)),

$$S(\%) = \frac{W_s - W_d}{W_d} \times 100 \quad (2)$$

where W_s and W_d are swollen and dry weight of samples, respectively. Pre-weighed dry films of the hydrogels were immersed in DI water at room temperature for 5 days. The weight of the swollen samples was measured after blotting excessive water gently with filter paper.

Mechanical testing of the swollen hydrogels at equilibrium was performed with the parallel plate compression geometry of the RSAIII Dynamic Mechanical Analyzer (DMA) with a 3.5 kg load cell. Using a cork borer, hydrogel samples of approximately 1 mm thickness were cut into disks of 6.7 mm diameter. Equilibrium swollen samples were kept in deionized water until mechanical testing. To prevent water loss during testing, hydrogel samples were immersed in DI water. Frequency dependent storage modulus (E') and loss modulus (E'') of each hydrogel were evaluated at room temperature at a compression frequency of 0.1–80 Hz with 0.1% strain amplitude. 0.2 N static force was applied to ensure the surface contact between hydrogel and upper compression plate. Compressive stress relaxation tests were carried out to evaluate time-dependent properties of equilibrium swollen hydrogels. For this purpose, equilibrium swollen hydrogel disks immersed in DI water were instantly compressed to 20% strain for 20 min and relaxation stress as a function of time was recorded. Relative relaxation rate and relative residual stress of hydrogels after 20 min were compared.

The number of effectively crosslinked chains per unit volume was calculated by using Eq. (3) (Anseth, Bowman, & Bannon-Peppas, 1996);

$$V_e = \frac{G}{RT\upsilon_2^{1/3}} \quad (3)$$

where V_e is the effective crosslink density in mol/cm^3, υ_2 the polymer volume fraction at equilibrium swollen state (reciprocal of Q), G the shear elastic modulus, R the gas constant, and T the temperature in Kelvin. Q, volume swelling ratio, was calculated from the weight swelling ratio (S). The relationship between the number of effectively cross-linked chains per unit volume (V_e) and the average

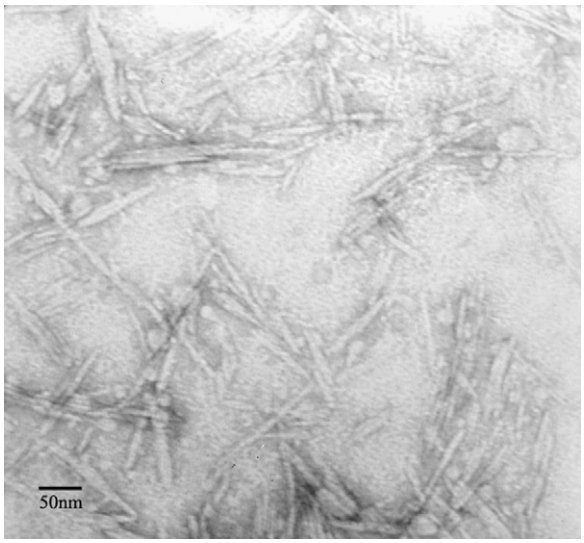

Fig. 1. TEM images of cellulose whiskers isolated from aspen wood pulp.

molecular weight between crosslinks ($\overline{M_C}$, g/mol) can be defined by Eq. (4),

$$\frac{\rho}{\overline{M_C}} = V_e \tag{4}$$

where ρ is the density of the polymer in the swollen gel (1.27 g/cm^3) (Corkhill, Jolly, Ng, & Tighe, 1987). G was determined by plotting σ versus (λ–λ^{-2}) and calculating the slope from the linear region of these curves. Here, σ is the compressive force per unit of the initial cross-sectional area of the swollen gel and λ is the deformation ratio (L/L_0) where L_0 and L is the thickness of the sample before and after the compression.

3. Results and discussion

3.1. Cellulose nanowhiskers

TEM images of cellulose nanowhiskers (CNW) isolated from aspen wood and filter paper by sulfuric acid hydrolysis are shown in Fig. 1. Hydrolysis of aspen wood yielded shorter nanocrystals but with slightly higher aspect ratios compared to filter paper CNW. Average length and diameter of CNW from aspen wood was $L = 156 \pm 19$ nm and $d = 11 \pm 3$ nm, while particles from filter paper had slightly larger dimensions ($L = 177 \pm 33$ nm, $d = 15 \pm 3$ nm); however, the average aspect ratio was comparable (14 and 12 for aspen wood and filter paper CNW, respectively). It is possible that the nanocrystals from aspen were smaller due to the lower crystallinity of aspen cellulose ($I = 53$–80%) (Beck-Candanedo et al., 2005), compared to the crystallinity of cellulose from filter paper ($I \approx 90\%$) (Park, Johnson, Ishizawa, Parilla, & Davis, 2009).

3.2. Hemicellulose isolate

From the aliphatic NMR spectrum (Fig. 2a), it is evident that this fraction did not contain any lignin, cellulose, mannan or arabinan. Present were the xylan (X) and 4-*O*-methyl-α-D-glucuronic acid (MeGA) correlations that are the most intense contours in the spectra. The X assignments were made for X-2 (3.13/72.4 ppm), X-3 (3.41/73.3 ppm), X-4 (3.64/76.1 ppm) and X-5a, X-5b (3.23, 3.96/62.6 ppm). The MeGA assignments were made for MeGA-2 (3.43/70.8 ppm), MeGA-3 (3.61/71.9 ppm), MeGA-4 (3.06/82.2 ppm), MeGA-5 (4.19/71.8 ppm), and MeGA–OCH_3 (3.32/59.6 ppm). A tentative correlation was assigned to the α-D-galactan (Ga) 6-position (3.62/61.1 ppm), suggesting that some galactan was retained in the hemicellulose isolate. Correlations attributed to X units that have a MeGA substituent (X-MeGA) were observed, but they displayed significantly less intense contours. Tentative assignments of the X-MeGA were made for X-MeGA-2 (3.28/76.1 ppm), X-MeGA-4 (4.00/80.2 ppm) and X-MeGA-5 (3.15, 3.83/64.9 ppm). Notably absent are the correlations for all *O*-acetylated xylan and mannan units, thus confirming that the *O*-acetyls were completely cleaved during the isolation process. The polysaccharides present in the hemicellulose isolate were also confirmed by the anomeric spectrum (Fig. 2b). The anomeric correlations for X (4.25/101.7 ppm) and MeGA (4.95/97.6 ppm) are easily assigned. The X-MeGA correlation is tentatively assigned at 4.49/100.5 ppm. The α and β reducing ends of X are visible at (5.05/91.9 ppm) and (4.22/98.1 ppm), respectively. The presence of Ga units is evidenced by their anomeric correlations for the terminal α-Ga (4.62/97.4 ppm) and terminal β-Ga (4.39/105.3 ppm) units, suggesting that this may either be a contaminant in the isolate or that Ga units are possibly incorporated to some degree along the xylan chain. Integration of the X-1 and MeGA-1 correlations in the HSQC spectra of the hemicellulose isolate suggested that the xylan had approximately one glucuronic acid substituent per 25 xylose units, and also that the MeGA substituent was entirely (1 → 2)-linked to the xylan chain.

Size exclusion chromatography of the hemicellulose isolate showed two broad peaks. Their apparent molecular weights, $M_p \approx 401{,}000$ and $391{,}000\ g\ mol^{-1}$, were determined by means of Pullulan calibration standards. Sugar analysis of the acid hydrolysate of the isolate showed that it consisted of approximately 70% xylan, 0.93% glucan, 0.48% galactan, and 0.29% mannan, which was consistent with the results of the two-dimensional NMR experiments. The abbreviated structure of the hemicellulose isolate is shown below:

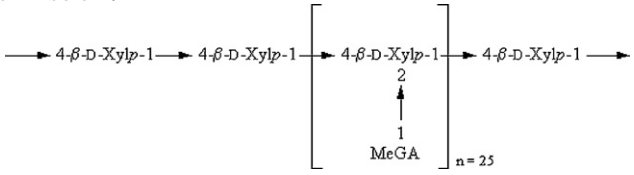

MeGA represents 4-*O*-methyl-α-D-glucuronic acid and "*n*" represents the number of Xyl*p* residues before the next expected MeGA substituent.

3.3. Methacrylation of hemicelluloses

Methacrylation of hemicellulose derived from aspen was confirmed by FT-IR analysis (Fig. 3b). After methacrylation peaks appeared at 1751 cm^{-1} (glucuronic acid ester C=O), 1713 cm^{-1} (methacrylic ester C=O), and 1635 cm^{-1} (methacrylic C=C). The degree of modification as determined by ^{1}H NMR was found to be 8% and 18% for MH-10 and MH-25, respectively. Both MH-10 and MH-25 were water-soluble which was advantageous for the adsorption experiments which were performed in aqueous medium.

3.4. Adsorption of MH to CNW

It has been proposed that the strength and interfacial stability of the plant cell wall is due to the unique network structure of cellulose microfibrils coated with other matrix poly- and hetero-saccharides (Teeri, Brumer, Daniel, & Gatenholm, 2007). The hemicelluloses self-assemble onto cellulose microfibrils and form interconnecting networks with other cell wall polymers (lignin, pectin), which results in the load-bearing ability of the plant cell

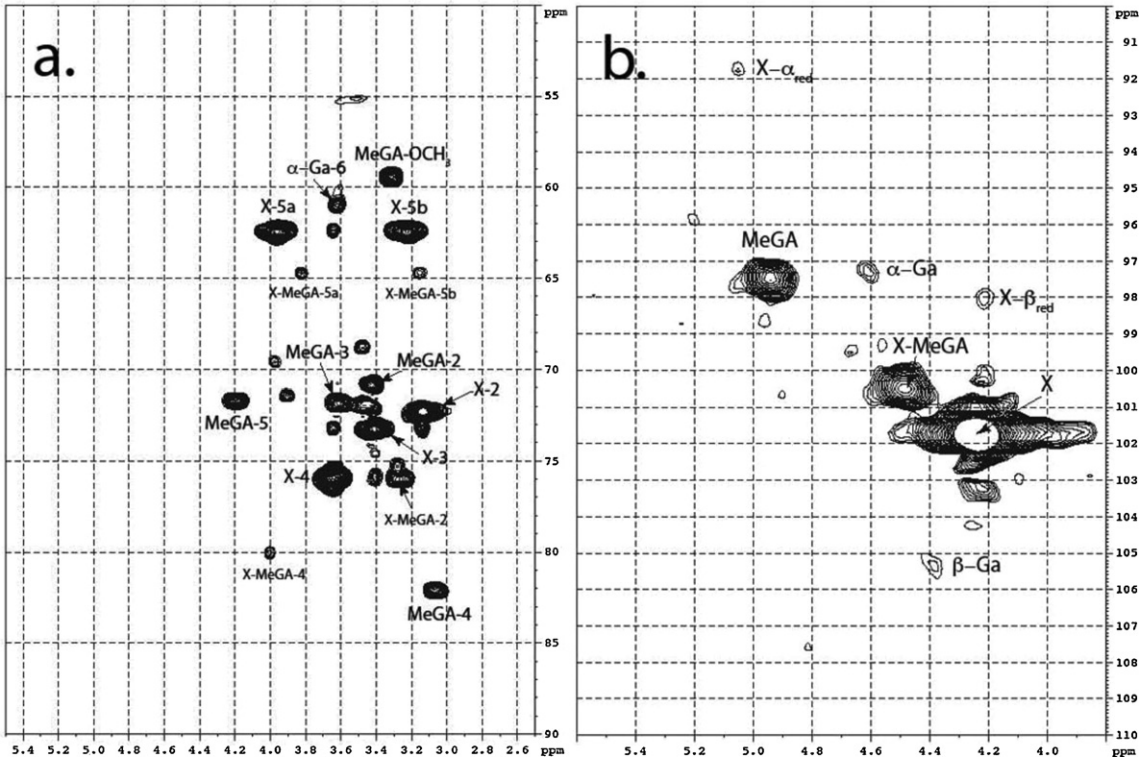

Fig. 2. HSQC spectra of the hemicellulose isolate; (a) aliphatic and (b) anomeric region of the isolate. For the spectra shown, the solvent was D_2O. The labels correspond to the following structures: X, internal β-D-xylopyranosyl units; G, internal β-D-glucopyranosyl units; MeGA, 4-*O*-methyl-α-D-glucuronic acid; X-MeGA, xylose units that are (1 → 2)-linked to MeGA; Ga, terminal D-galactopyranosyl units.

wall (Carpita & Gibeaut, 1993). Based on these assumptions, the natural intrinsic affinity of hemicelluloses for cellulose was used in this study to attach hemicellulose modified with methacrylic functionalities to the CNW surfaces. The "grafting from" approach on cellulose whiskers was then used to synthesize nanoreinforced hydrogels by *in situ* free radical polymerization of methacrylic functionalities immobilized on the CNW surfaces by the adsorbed hemicellulose.

Adsorption of hardwood hemicelluloses (glucoronoxylans) onto cellulose substrates have been shown to be dependent on several parameters, such as xylan molecular structure, xylan concentration, crystallinity and the surface area of cellulose substrate, time, temperature, pH of the solution (Henriksson & Gatenholm, 2001). High xylan concentration in the solution, low xylan substitution pattern (branching), high cellulose crystallinity, large surface area of the cellulose substrate, high temperatures and the prolonged processing time have been reported to increase the hemicellulose adsorption (Köhnke, 2010). To date, most of the adsorption experiments were conducted under autoclave conditions at high temperatures and alkaline pH (Linder & Gatenholm, 2004). Moreover, the number of studies on the adsorption of hemicelluloses to cellulose nanocrystals has been very limited (Bodin et al., 2007; Zhou, Brumer, & Teeri, 2009).

In this study, the adsorption of MH on CNW was performed under mild conditions (45 °C for 24 h) in order to prevent the possible cleavage (de-esterification) of surface sulfate groups on CNW. It has been reported that sulfate groups on CNW surface are stable up to 50 °C but susceptible to detachment at higher temperatures which results in further degradation/hydrolysis of the CNW (Pranger & Tannenbaum, 2008). Solvent exchange resulting in CNW organogels is essential to enable hydrogen bonds among whiskers to be formed. It has been shown that a polymer solution which is normally immiscible with CNW could fill the solvent-exchanged CNW network (Capadona et al., 2007). Moreover, the CNW organogel could be easily redispersed in water without forming CNW aggregates.

The adsorption of MH was verified by FT-IR analysis. Besides the typical peaks for cellulose, additional peaks, characteristic of methacrylates appeared at 1751 cm^{-1}, 1713 cm^{-1} and 1635 cm^{-1} indicating the presence of MH on the CNW. TEM micrographs did not show any significant difference in morphology or dispersion of CNW after coating with MH.

Colorimetric iodine-complexation showed that 70% and 74% of the originally added MH was adsorbed to CNW for MH-25 and MH-10, respectively. Compared to the results reported in literature (Henriksson & Gatenholm, 2001; Köhnke, 2010), the percentage of adsorbed hemicellulose was relatively high with respect to the processing temperature. This might be due to the comparatively larger surface area and the higher crystallinity of CNW used in this study as compared to CNW from other cellulose substrates (Morandi, Heath, & Thielemans, 2009; Samir et al., 2005; Sturcova, Davies, & Eichhorn, 2005). MH-10, which had a lower degree of modification than that of MH-25 and therefore probably had less branching on the hemicellulose backbone, adsorbed slightly more in comparison to MH-25. This result was consistent with the fact that the hemicellulose molecules with longer unsubstituted segments were preferentially adsorbed on cellulose surfaces; in addition, increased amount of branching on the hemicellulose backbone could impact the reaction of iodine with hemicellulose and thus result in less coloration (Köhnke et al., 2009; Gaillard & Thompson, 1971)

3.5. Synthesis and network structure of nanoreinforced hydrogels

Nanoreinforced PHEMA hydrogels (NR-PHEMA) were prepared by *in situ* free radical polymerization of HEMA

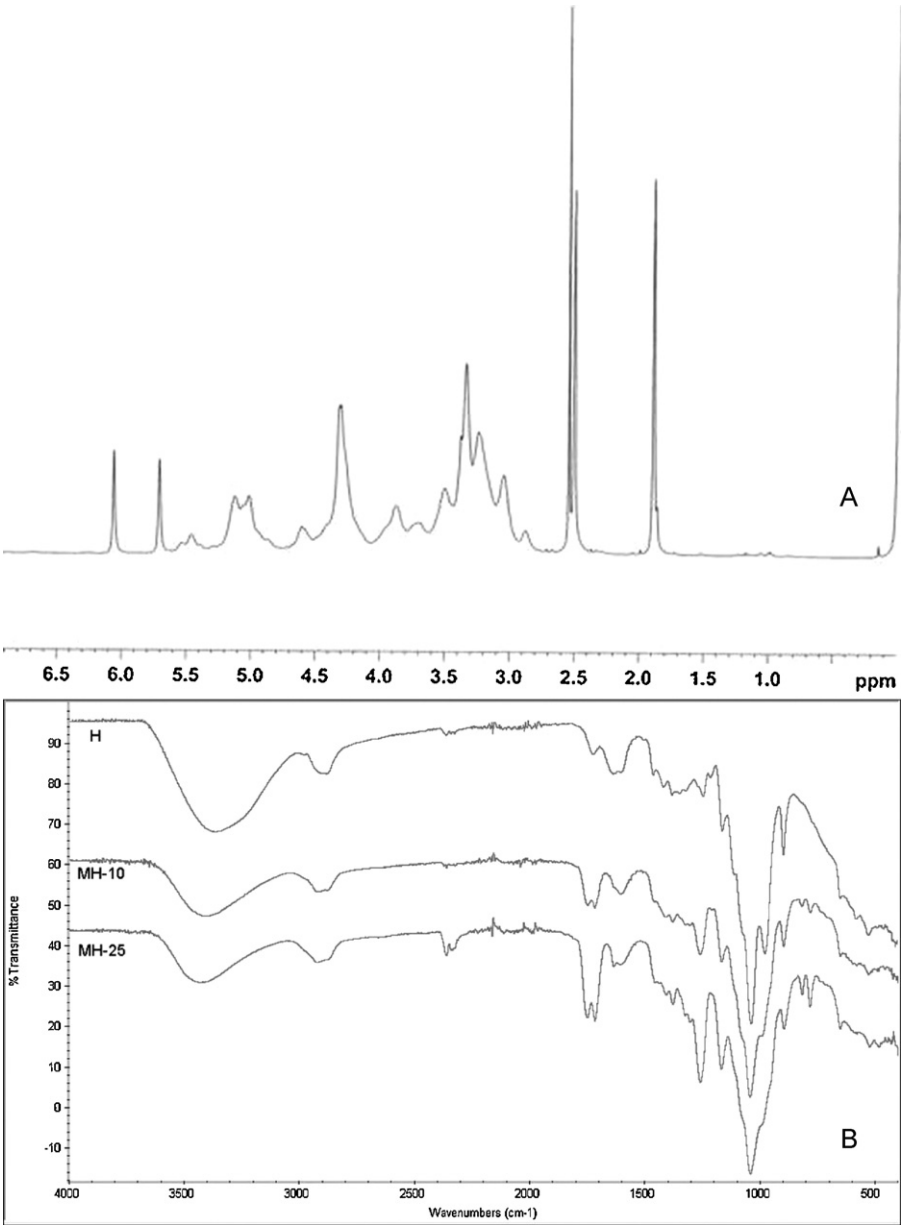

Fig. 3. (a) ^{1}H NMR spectra of methacrylated hemicelluloses (MH-25). New peaks appeared: 6.07 ppm (s, 1H, vinyl C–H); 5.70 ppm (s, 1H, vinyl C–H); 4.31 ppm (m, 4H, CH_2O); 1.89 ppm (s, 3H, CH_3). (b) FTIR spectra of hemicelluloses (H: unmodified; MH-10 and MH-25: methacrylated for 10 h and 25 h, respectively).

monomer in the presence of aqueous dispersion of CNW coated with MH.

The hypothesis was to use MH-coating on CNWs to create multifunctional crosslinking points and to grow PHEMA polymer chains on and in-between individual CNWs. Uniform dispersion of CNWs in aqueous medium could be achieved by the repulsion of negatively charged surface sulfate groups. The double bonds at the surface of CNWs introduced through the MH layer are proposed to be grafting sites for PHEMA polymer chains. A possible mechanism for the formation of the hydrogel is shown in Fig. 4. The potential hydrogel network structure could then contain crosslinked chains connecting two CNW to each other; short polymer chains with one end attached to the surface of a CNW and the other chain end moving freely; looped chains; entangled chains; and ungrafted free chains. It has been shown that for the mechanical properties of NC and MMC gels to be acceptable, a significant amount of crosslinked chains per unit volume must be formed (Haraguchi & Takehisa, 2002b; Haraguchi, Farnworth, Ohbayashi, & Takehisa, 2003; Huang et al., 2007). Moreover, Goetz, Mathew, Oksman, Gatenholm, & Ragauskas (2009) have shown that *in situ* co-crosslinking of CNWs with a polymer matrix could maintain uniform dispersion of CNWs in the matrix and yield a homogeneous hydrogel network with unique water absorbing properties. It was shown that crosslinking the matrix polymer with CNWs prevented nanowhiskers aggregation and enhanced the mechanical properties of the nanocomposite (Goetz, Foston, Mathew, Oksman, & Ragauskas, 2010). The mechanical properties were found to be dependant on the degree of crosslinking (or the amount of crosslinking chains) and could be improved with increasing CNW content.

3.6. Mechanical properties

Fig. 5a shows the typical stress–strain curves of NR-PHEMA and control NS-PHEMA hydrogels obtained from uniaxial unconfined compression tests. Under the chosen conditions, the maximum amount of stress that could be applied was about 800 KPa. At that

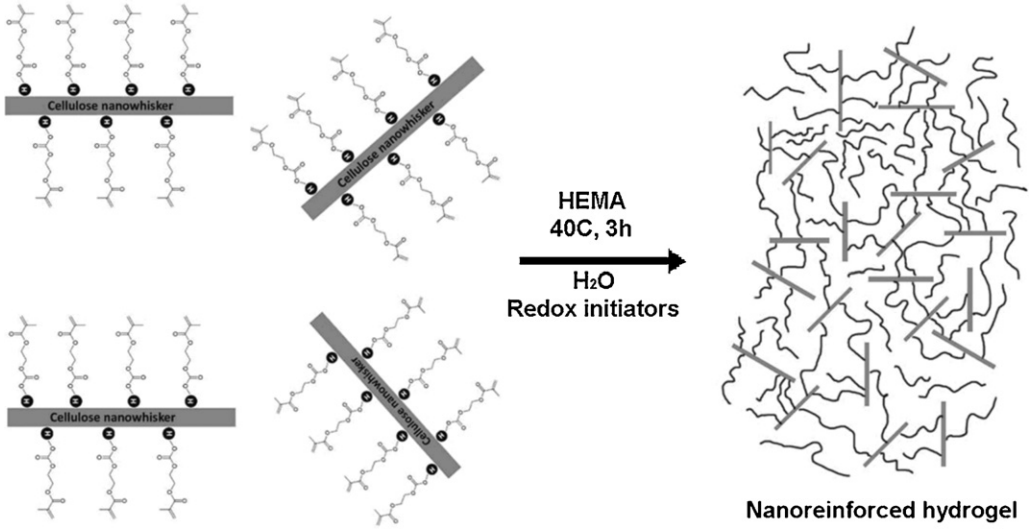

Fig. 4. Proposed mechanism for the formation of nanoreinforced PHEMA hydrogel.

stress level, no fracture or break was observed in any of the hydrogel samples. The strain at that stress level and the elastic moduli calculated from the stress–strain curves are given in Table 1. To evaluate the transition of the modulus (E) in the highly non-linear stress–strain curves, the average tangent slope at 10% strain increments from 10 to 90% strain was calculated (Fig. 5b) (Stammen, Williams, Ku, & Guldberg, 2001).

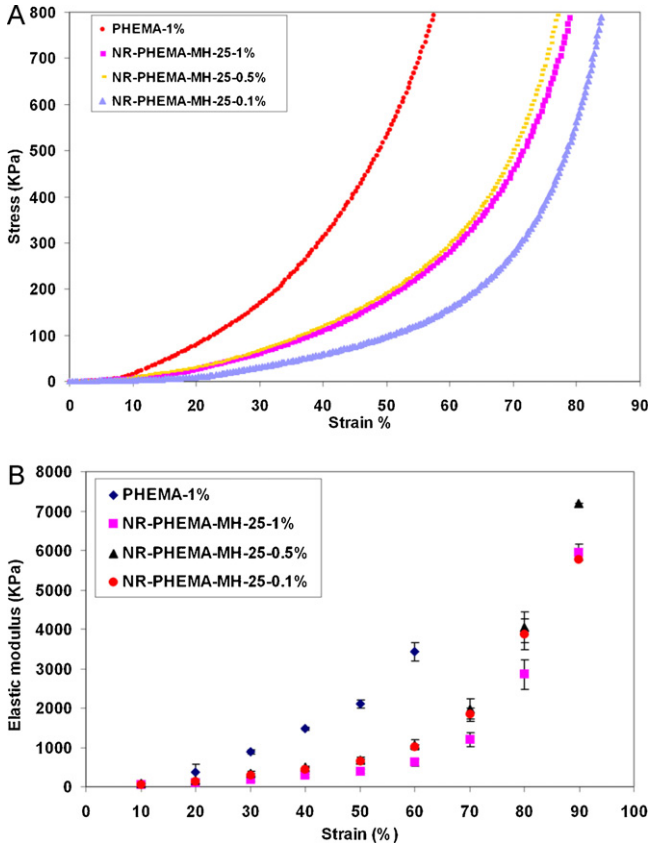

Fig. 5. (a) Typical stress strain curves of NR-PHEMA hydrogels reinforced with different weight fractions (0.1%, 0.5% and 1%, w/w) of CNW coated with MH-25 and (b) average tangent elastic modulus at 10% strain increments calculated from stress strain curves. Control sample is NS-PHEMA hydrogel crosslinked with 1% (w/w) EGDMA.

Observed J-shaped curves indicating low modulus at low strains and high modulus at high strains with an instantaneous transition implied increased toughness and strength in hydrogels designed for load-bearing applications. This behavior is characteristic of many biological tissues that can be considered as natural gels (Calvert, 2009).

Compared to control NS-PHEMA hydrogels, the transition from low to high modulus was more pronounced for NR-PHEMA gels. Fig. 5b and Table 1 show the transition of compressive tangent modulus (E) with increasing compressive strain. Within 10–60% strain, the modulus of the control gels was 3–5 times higher than that of NR-PHEMA. To better understand the results, the network parameters for each hydrogel were calculated according the rubber elasticity theory (see Table 2).

In chemically crosslinked hydrogels with conventional crosslinkers, the distribution of chain lengths usually is broad due to the random distribution of crosslinking points (Huang et al., 2007). This might result in the formation of large amounts of short chains with restricted mobility. Therefore, stress built up in the control NS-PHEMA gels might have been higher than in comparable NR-PHEMA. This phenomenon was in accordance with the average molecular weight between crosslinks ($\overline{M_c}$) calculated for the control samples which was 4–9 fold lower than that of NR-PHEMA gels. However, overall $\overline{M_c}$ values were rather high (up to about 130,000 g/mol) for NR-PHEMA and thus the modulus of NR-PHEMA low compared to control hydrogels because of the presence of long flexible polymer chains between crosslinking points and the high mobility of these polymer chains in the water-swollen state. Accordingly, NR-PHEMA gels showed elongation up to about 80% while the controls only amounted to 59% at comparable stress level (see Table 1). However, modulus values increased instantaneously when the strain was increased further. Surprisingly, tangent modulus values of NR-PHEMA gels above 80% strain were 5–19 times higher than at 60%. Moreover, the modulus of NR-PHEMA gels ranged from 5.6 to 6.8 MPa (control samples only about 3.4 MPa). A possible explanation for this sudden increase in modulus might be the restriction of the mobility of the long polymer chains in NR-PHEMA gels. The polymer chains between crosslinks were probably close to their full extension and their mobility was restricted because the water inside the hydrogels was squeezed out. It needs to be emphasized that no visible fracture could be detected even at this high compression and the samples recovered to their original shape when the force was removed.

Table 1
The average and standard deviation values of compressive strain (ε), tangent modulus (E) and shear modulus (G) of hydrogels.

	ε (%) at 800 KPa	E (KPa) at ε = 60%	E (KPa) at $\varepsilon \geq 80\%$	G (KPa)
NS-PHEMA(control)	59 ± 1.4	3434 ± 239	N/A	156 ± 5.3
NR-PHEMA-MH-10-0.1%	82 ± 1.4	847 ± 46	5661 ± 135	27 ± 4.0
NR-PHEMA-MH-10-0.5%	81 ± 1.1	913 ± 56	6593 ± 65	31 ± 3.5
NR-PHEMA-MH-10-1%	86 ± 0.3	355 ± 13	6791 ± 51	16 ± 0.8
NR-PHEMA-MH-25-0.1%	79 ± 1.6	1023 ± 44	5763	35 ± 5.1
NR-PHEMA-MH-25-0.5%	78 ± 2.0	1070 ± 134	N/A	40 ± 7.3
NR-PHEMA-MH-25-1%	84 ± 1.6	618 ± 93	5956 ± 208	19 ± 4.3

N/A = Not available.

3.6.1. Effect of the degree of modification of hemicellulose

Assuming that the amount of MH coated per unit gram of CNW (140–150 mg/g) was approximately the same for MH-10 and MH-25, the influence of the degree of methacrylation on the mechanical properties of NR-PHEMA gels was evaluated. Tangent modulus values at 60% strain revealed that NR-PHEMA gels reinforced with MH-25 coated CNWs resulted in higher modulus compared to gels reinforced with MH-10 coated CNWs. This result was consistent for each CNW weight fraction used in this study. G values followed the same trend as well, although less pronounced.

One possible explanation for this trend might be the increase in crosslink density with increasing methacrylic functionality at the surface of CNW. As can be seen in Table 2, for the same CNW weight fraction, V_e values were slightly higher for samples loaded with MH-25 coated CNW. It is likely that with increased amount of double bonds at the surface of CNW, the number of PHEMA polymer chains grafted from each CNW and the number of crosslinking chains connecting adjacent CNWs increased. As a result, the average length of the polymer chains between crosslinking points decreased (see $\overline{M_c}$ values in Table 2). This may have resulted in the formation of a denser network with shorter/more crosslinks.

3.6.2. Effect of CNW concentration

The concentration of MH coated CNW in the NR-PHEMA hydrogels was 0.1%, 0.5% and 1% (w/w) with respect to the amount of HEMA monomer used for the polymerization. It was hypothesized that a decrease of the $\overline{M_c}$ could also be achieved by increasing the concentration of the CNW.

For both MH-10 and MH-25 coated CNW, as the CNW concentration increased, calculated $\overline{M_c}$ values decreased to some extent which was in accordance with the outlined hypothesis. As a result, both tangent and shear moduli increased slightly with increasing CNW content. However, further increase in the CNW content to 1% (w/w) resulted in an unexpected increase in $\overline{M_c}$ and consequently a decrease in modulus.

Since the polymer chains in NR-PHEMA gels are fairly large and mobile, it has been suggested that the water content of hydrogels could have a similar effect as temperature has on glassy polymers (Calvert, 2009). Therefore, flexible polymer chains of swollen hydrogels could behave like glassy polymers above their glass transition temperature (Haraguchi et al., 2002). In NR-PHEMA gels with 1% CNW content, the swelling ratios were high probably due to the hydrophilic groups introduced through cellulose and hemicellulose (see Table 2). Higher water content then resulted in lower modulus values and more rubber-like behavior. When the water content in all NR-PHEMA hydrogels was comparable, modulus values therefore increased with increasing CNW content (see Table 1). This result is in accordance with observations of mechanical properties at higher compressive strains ($\varepsilon \geq 80\%$) when most of the water had been forced out.

Table 2
Average chain lengths between crosslinks ($\overline{M_c}$), the number of effective crosslinking chains (V_e) and swelling ratios (S) of hydrogels.

	$\overline{M_c}$ (g/mol)	V_e (10^5 mol/cm^3)	S (%)
NS-PHEMA(control)	15,984	7.9	70 ± 2.4
NR-PHEMA-MH-10-0.1%	87,210	1.5	92 ± 2.6
NR-PHEMA-MH-10-0.5%	79,964	1.6	81 ± 6.7
NR-PHEMA-MH-10-1%	139,822	0.9	128 ± 8.4
NR-PHEMA-MH-25-0.1%	69,154	1.8	81 ± 4.1
NR-PHEMA-MH-25-0.5%	61,717	2.1	80 ± 4.6
NR-PHEMA-MH-25-1%	123,677	1.0	95 ± 2.5

3.6.3. Stress relaxation

Fast relaxation rate and low residual stress obtained from a stress relaxation test indicate high degree of recovery, good resilience and increased viscoelasticity (Millon et al., 2009; Lv et al., 2010). Despite the high compressive strains up to about 80% NR-PHEMA hydrogels completely recovered to their original dimensions once the force was lifted. To further evaluate the time-dependent mechanical properties and the degree of the recovery of the hydrogels, stress relaxation tests were performed. In Fig. 6 the relative residual stress is graphed as a function of time with respect to initial stress.

Stress relaxation behavior of control NS-PHEMA and NR-PHEMA hydrogels were significantly different. The relaxation rate of NR-PHEMA was apparently fast and the relative stress remaining after 20 min was quite low compared to that of control gels. NR-PHEMA gels had dissipated 80% of the stress within 6–13 s, compared to 460 s in case of the controls. The residual stress in the control gels remained at 77% of the initial stress and reached a plateau. In comparison, in NR-PHEMA gels the residual stress was only 11%. The observed recovery properties of NR-PHEMA gels may be due to the proposed network structure composed of long flexible PHEMA chains between uniformly distributed crosslinking points which would ease the distribution of the applied force.

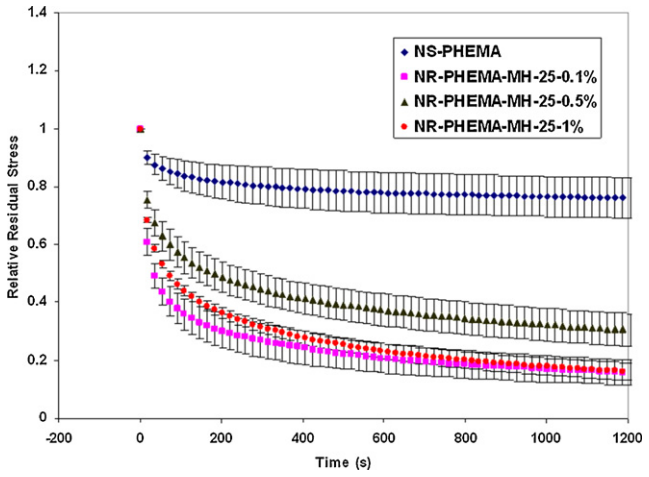

Fig. 6. Change in the relative residual relaxation stress with time for NS-PHEMA and NR-PHEMA hydrogels reinforced with different weight fractions of CNW coated with MH-25. Error bars represents standard deviation.

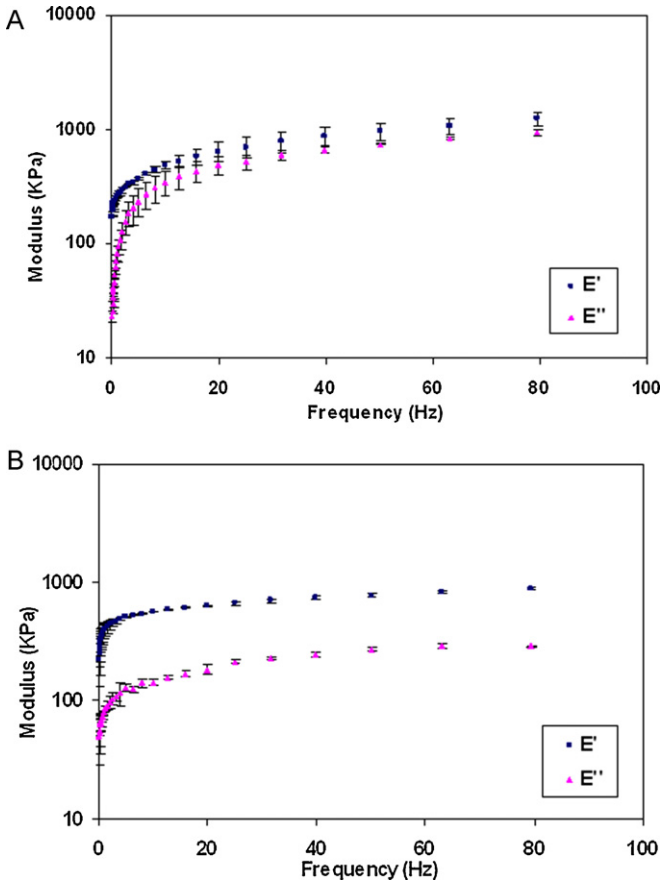

Fig. 7. Storage (solid-line) and loss (dashed-line) modulus as a function of frequency for hydrogels (a) control NS-PHEMA hydrogel crosslinked with 1% (w/w) EGDMA. (b) NR-PHEMA including 1% (w/w) CNW coated with MH-25. Error bars represents standard deviation.

3.6.4. Dynamic viscoelastic properties

Dynamic mechanical analysis is a nondestructive method used to characterize the viscoelastic properties of materials. An oscillatory strain or stress is applied to a material, resulting in stress or strain that can be measured. The response of a material to a sinusoidally varying force as a function of frequency or temperature is defined by the storage modulus, loss modulus and loss tangent. Storage modulus (E') represents the elastic response of a material and is proportional to the energy stored. Loss modulus (E'') represents the viscous response of the material and is proportional to the energy dissipated as heat. Loss tangent ($\tan\delta$) is the ratio of energy loss to energy stored (E''/E') (Jones, 1999).

NR-PHEMA hydrogels showed viscoelastic behavior evidenced by non-linear stress–strain response and time-dependant stress relaxation. Frequency sweep tests were performed to evaluate the dependence of modulus (E'' and E') on loading frequency. Frequency was scanned between 0.1 and 80 Hz which has been reported to cover all physiological loading frequency in the human body during daily activities (Meakin, Hukins, Aspden, & Imrie, 2003). Fig. 7 shows the viscoelastic behavior of control NS-PHEMA and NR-PHEMA gels including 1% (w/w) CNW coated with MH-25. The E' and E'' values of control gels increased with increasing frequency and the value of E'' approached the value of E'. The increase in the value of E'' means that the amount of energy dissipated as heat is significant due to the increased friction among polymer chains (Hafeman et al., 2008). However, NR-PHEMA gels showed different viscoelastic behavior. The value of E' slightly increased and reached a plateau at higher frequencies. The value of E'' was much lower than that of E' over all frequencies and showed less dependency on frequency compared to that of NS-PHEMA gels. Obviously, more energy was stored in NR-PHEMA gels rather than dissipated as heat which would be a characteristic behavior of an ideal elastomer in its rubbery state (Fulcher, Hukins, & Shepherd, 2009). It is possible that there was less internal friction between polymer chains in NR-PHEMA gels as a consequence of its unique network structure. This might be the reason why NR-PHEMA gels relaxed faster to lower stresses and therefore had improved recovery.

3.7. Swelling

The water uptake of hydrogels in their equilibrium swollen state is shown in Table 2. NR-PHEMA gels had slightly higher swelling ratios (80–128%) compared to control NS-PHEMA gels (70%). With increased concentration of MH coated CNW, swelling ratio increased which might be as a result of the additional H-bonding between hydrophilic groups introduced by cellulose and hemicellulose. However, for the same CNW weight fraction, NR-PHEMA gels from MH-25 had lower swelling ratios. Considering the $\overline{M_c}$ values given in Table 2, it is clear that the network parameters had a direct influence on the swelling ratios. With decreasing crosslink density and increasing $\overline{M_c}$, swelling ratios increased because more space was available for water molecules in the hydrogel network.

4. Conclusions

In summary, a novel strategy was developed to synthesize hydrogels based on cellulose nanowhiskers and hemicellulose isolated from wood. Hemicellulose was functionalized using a "grafting from" approach to attach methacrylic functional groups for polymerization and network formation. Utilizing its inherent affinity, hemicellulose was then deposited on the surface of individual cellulose whiskers to create multifunctional crosslinking sites. Network structure, mechanical, viscoelastic and swelling properties of the synthesized PHEMA hydrogels were dependent on the degree of modification of the hemicellulose and the cellulose nanowhisker content. Toughness, extensibility as well as recovery properties of nanoreinforced PHEMA hydrogels were superior to those prepared using conventional crosslinking agents. Overall, the characteristics of the produced PHEMA hydrogels, such as water holding capacity, mechanical properties and viscoelasticity, appeared to be similar to load-bearing natural tissue having hydrogel-like characteristics. Therefore, they might be considered as potential replacement materials for articular cartilage.

Acknowledgement

The authors are grateful for the financial support of the Wood Education and Resource Center (WERC).

References

Anseth, K. S., Bowman, C. N., & Bannon-Peppas, L. (1996). Mechanical properties of hydrogels and their experimental determination. *Biomaterials*, *17*, 1647–1657.

Araki, J., Wada, M., Kuga, S., & Okano, T. (1998). Flow properties of microcrystalline cellulose suspension prepared by acid treatment of native cellulose. *Colloids and Surfaces A: Physicochemical and Engineering Aspects*, *142*, 75–82.

Beck-Candanedo, S., Roman, M., & Gray, D. G. (2005). Effect of reaction conditions on the properties and behavior of wood cellulose nanocrystal suspensions. *Biomacromolecules*, *6*, 1048–1054.

Bodin, A., Ahrenstedt, L., Fink, H., Brumer, H., Risberg, B., & Gatenholm, P. (2007). Modification of nanocellulose with a xyloglucan–RGD conjugate enhances adhesion and proliferation of endothelial cells: Implications for tissue engineering. *Biomacromolecules*, *8*, 3697–3704.

Boschetti, F., Pennati, G., Gervaso, F., Peretti, G. M., & Dubini, G. (2004). Biomechanical properties of human articular cartilage under compressive loads. *Biorheology*, *41*, 159–166.

Bryant, S. J., Janet, L. C., Hauch, K. D., & Ratner, B. D. (2007). Photo-patterning of porous hydrogels for tissue engineering. *Biomaterials*, *28*, 2978–2986.
Calvert, P. (2009). Hydrogels for soft machines. *Advanced Materials*, *21*, 743–756.
Capadona, J. R., Van Den Berg, O., Capadona, L. A., Schroeter, M., Rowan, S., Tyler, D. J., et al. (2007). A versatile approach for the processing of polymer nanocomposites with self-assembled nanofibre templates. *Nature Nanotechnology*, *2*, 765–769.
Carpita, N. C., & Gibeaut, D. M. (1993). Structural models of primary cell walls in flowering plants: Consistency of molecular structure with the physical properties of the walls during growth. *The Plant Journal*, *3*, 1–30.
Corkhill, P. H., Jolly, A. M., Ng, C. O., & Tighe, B. J. (1987). Synthetic hydrogels: 1. Hydroxyalkyl acrylate and methacrylate copolymers—Water binding studies. *Polymer*, *28*, 1758–1766.
Dong, M. X., Revol, J. F., & Gray, D. G. (1998). Effect of microcrystallite preparation conditions on the formation of colloid crystals of cellulose. *Cellulose*, *5*, 19–32.
Ebringerova, A. (2006). Structural diversity and application potential of hemicelluloses. *Macromolecular Symposia*, *232*, 1–12.
Fulcher, G. R., Hukins, D. W. L., & Shepherd, D. E. T. (2009). Viscoelastic properties of bovine articular cartilage attached to subchondral bone at high frequencies. *BMC Musculoskel Disorders*, *10*, 61–68.
Gaillard, B. D. E., & Thompson, N. S. (1971). Interaction of polysaccharides with iodine, Part II. The behavior of xylans in different salt solutions. *Carbohydrate Research*, *18*, 137–146.
Gatenholm, P., & Tenkanen, M. (2004). *Hemicelluloses: Science and Technology*. New York: Oxford University Press.
Goetz, L., Mathew, A., Oksman, K., Gatenholm, P., & Ragauskas, A. J. (2009). A novel nanocomposite film prepared from crosslinked cellulosic whiskers. *Carbohydrate Polymers*, *75*, 85–89.
Goetz, L., Foston, M., Mathew, A. P., Oksman, K., & Ragauskas, A. J. (2010). Poly(methyl vinyl ether-co-maleic acid)-polyethylene glycol nanocomposites cross-linked in situ with cellulose nanowhiskers. *Biomacromolecules*, *11*, 2660–2666.
Gröndahl, M., Teleman, A., & Gatenholm, P. (2003). Effect of acetylation on the material properties of glucuronoxylan from aspen wood. *Carbohydrate Polymers*, *52*, 359–366.
Habibi, Y., Lucia, L. A., & Rojas, O. J. (2010). Cellulose nanocrystals: Chemistry, self-assembly, and applications. *Chemical Reviews*, *110*(6), 3479–3500.
Hafeman, A. E., Li, B., Yoshii, T., Zienkiewicz, K., Davidson, J. M., & Guelcher, S. A. (2008). Injectable biodegradable polyurethane scaffolds with release of platelet-derived growth factor for tissue repair and regeneration. *Pharmaceutical Research*, *10*, 2387–2399.
Haraguchi, K., & Takehisa, T. (2002). Nanocomposite hydrogels: A unique organic–inorganic network structure with extraordinary mechanical, optical, and swelling/de-swelling properties. *Advanced Materials*, *14*, 1120–1124.
Haraguchi, K., Takehisa, T., & Fan, S. (2002). Effects of clay content on the properties of nanocomposite hydrogels composed of poly(N-isopropylacrylamide) and clay. *Macromolecules*, *35*, 10162–10171.
Haraguchi, K., Farnworth, R., Ohbayashi, A., & Takehisa, T. (2003). Compositional effects on mechanical properties of nanocomposite hydrogels composed of poly(N,N-dimethylacrylamide) and clay. *Macromolecules*, *36*, 5732–5741.
Henriksson, Å., & Gatenholm, P. (2001). Controlled assembly of glucuronoxylans onto cellulose fibres. *Holzforschung*, *55*, 494–502.
Huang, T., Xu, H., Jiao, K., Zhu, L., Brown, H. R., & Wang, H. (2007). A novel hydrogel with high mechanical strength: A macromolecular microsphere composite hydrogel. *Advanced Materials*, *19*, 1622–1626.
Jones, D. S. (1999). Dynamic mechanical analysis of polymeric systems of pharmaceutical and biomedical significance. *International Journal of Pharmaceutics*, *179*, 167–178.
Karaaslan, M. A., Tshabalala, M., & Buschle-Diller, G. (2010). Wood hemicellulose/chitosan-based semi-interpenetrating network hydrogels: Mechanical swelling and controlled drug release properties. *Bioresources*, *5*, 1036.
Köhnke, T. (2010). Adsorption of xylans on cellulosic fibres: Influence of xylan composition on adsorption characteristics and kraft pulp properties. Göteborg: Dissertation, Chalmers University of Technology.
Köhnke, T., Brelid, H., & Westman, G. (2009). Adsorption of cationized barley husk xylan on kraft pulp fibres: Influence of degree of cationization on adsorption characteristics. *Cellulose*, *16*(6), 1109–1121.
Lima, M. M. D., & Borsali, R. (2004). Rodlike cellulose microcrystals: Structure, properties, and applications. *Macromolecular Rapid Communications*, *25*, 771–787.
Lindblad, M. S., Ranucci, E., & Albertsson, A. (2001). Biodegradable polymers from renewable sources. New hemicellulose-based hydrogels. *Macromolecular Rapid Communications*, *22*, 962–967.
Lindblad, M. S., Albertsson, A. C., Ranucci, E., Laus, M., & Giani, E. (2005). Biodegradable polymers from renewable sources: Rheological characterization of hemicellulose-based hydrogels. *Biomacromolecules*, *6*, 684–690.
Linder, Å., & Gatenholm, P. (2004). Effect of cellulose substrate on assembly of xylan. In *Hemicelluloses: Science and technology*. New York: Oxford University Press., pp. 236–253, (Chapter 16).
Lv, S., Dudek, D. M., Cao, Y., Balamurali, M. M., Gosline, J., & Li, H. (2010). Designed biomaterials to mimic the mechanical properties of muscles. *Nature*, *465*, 69–73.
Meakin, J. R., Hukins, D. W. L., Aspden, R. M., & Imrie, C. T. (2003). Rheological properties of poly(2-hydroxyethyl methacrylate) (PHEMA) as a function of water content and deformation frequency. *Journal of Materials Science: Materials in Medicine*, *14*, 783–787.
Millon, L. E., Oates, C. J., & Wan, W. (2009). Compression properties of polyvinyl alcohol-bacterial cellulose nanocomposite. *Journal of Biomedical Materials Research Part B: Applied Biomaterials*, *90B*, 922–929.
Morandi, G., Heath, L., & Thielemans, W. (2009). Cellulose nanocrystals grafted with polystyrene chains through surface-initiated atom transfer radical polymerization (SI-ATRP). *Langmuir*, *25*, 8280–8286.
Park, S., Johnson, D. K., Ishizawa, C. I., Parilla, P. A., & Davis, M. F. (2009). Measuring the crystallinity index of cellulose by solid state ^{13}C nuclear magnetic resonance. *Cellulose*, *16*, 641–647.
Peppas, N. A., Hilt, J. Z., Khademhosseini, A., & Langer, R. (2006). Hydrogels in biology and medicine: from fundamentals to bionanotechnology. *Advanced Materials*, *18*, 1345.
Pranger, L., & Tannenbaum, R. (2008). Biobased nanocomposites prepared by in-situ polymerization of furfuryl alcohol with cellulose whiskers or montmorillonite clay. *Macromolecules*, *41*, 8682–8687.
Samir, M. A. S. A., Alloin, F., & Dufresne, A. (2005). Review of recent research into cellulosic whiskers, their properties and their application in nanocomposite field. *Biomacromolecules*, *6*(2), 612–626.
Saxena, A., Elder, T. J., Pan, S., & Ragauskas, A. J. (2009). Novel nanocellulosic xylan composite film. *Composites Part B: Engineering*, *40*, 727–730.
Saxena, A., Elder, T. J., & Ragauskas, A. J. (2011). Moisture barrier properties of xylan composite films. *Carbohydrate Polymers*, *84*, 1371–1377.
Slaughter, B. V., Khurshid, S. S., Fisher, O. Z., Khademhosseini, A., & Peppas, N. A. (2009). Hydrogels in regenerative medicine. *Advanced Materials*, *21*, 1.
Stammen, J. A., Williams, S., Ku, D. N., & Guldberg, R. E. (2001). Mechanical properties of a novel PVA hydrogel in shear and unconfined compression. *Biomaterials*, *22*, 799–806.
Sturcova, A., Davies, G. R., & Eichhorn, S. J. (2005). Elastic modulus and stress-transfer properties of tunicate cellulose whiskers. *Biomacromolecules*, *6*, 1055–1061.
Teeri, T. T., Brumer, H., Daniel, G., & Gatenholm, P. (2007). Biomimetic engineering of cellulose-based materials. *Trends in Biotechnology*, *25*, 299–306.
Zhou, Q., Rutland, M. W., Teeri, T. T., & Brumer, H. (2007). Xyloglucan in cellulose modification. *Cellulose*, *14*, 625–641.
Zhou, Q., Brumer, H., & Teeri, T. T. (2009). Self-organization of cellulose nanocrystals adsorbed with xyloglucan oligosaccharide-poly(ethyleneglycol)-polystyrene triblock copolymer. *Macromolecules*, *42*, 5430–5432.